International Journal on Science and Technology (IJSAT)
E-ISSN: 2229-7677 ● Website: www.ijsat.org ● Email: editor@ijsat.org

Study of Structural and Optical Properties of WO_3- Polyaniline Thin films Developed by Chemical Bath Deposition Method

Satish S. Haral[1], Vijay S. Kale[2], D. K. Halwar[3]

Department of Electronic Science and Research Centre
MGV's L.V.H. ASC College, Nashik, Dist.-Nashik
Affiliated to Savitribai Phule Pune University, Maharashtra, India.

Abstract:
In the present research work, WO_3–Polyaniline (PANI) thin films were successfully prepared on glass substrates using the chemical bath deposition (CBD) method. The structural and optical properties of the films were systematically investigated using FESEM, EDX, XRD, FTIR, and UV–Vis spectroscopy. The XRD analysis revealed distinct diffraction peaks corresponding to monoclinic WO_3 (JCPDS No. 83-0950), along with a broad hump attributed to the semi-crystalline nature of PANI, confirming the formation of an organic–inorganic hybrid structure. The calculated average crystallite size was found to be approximately 15.6 nm, indicating the nanocrystalline nature of the composite film. FESEM images showed agglomerated nanostructures with irregular shapes and porous morphology, while the BET analysis estimated a specific surface area of 3.68 m^2/g, favoring enhanced interfacial interactions. EDX spectra confirmed the elemental composition with the presence of tungsten, oxygen, and carbon, validating the successful incorporation of WO_3 and PANI into the composite. FTIR analysis further supported the hybrid structure by identifying characteristic vibrational bands of both WO_3 (W–O–W stretching) and PANI (C–N, C=C, and N–H vibrations). Optical studies from UV–Vis spectroscopy revealed strong absorption in the UV–visible region, and the Tauc plot estimated the direct optical band gap to be 3.2 eV. The combined structural and optical outcomes demonstrate that WO_3–PANI thin films exhibit nanocrystalline, porous, and semiconducting features, making them promising candidates for optoelectronic, electrochromic, and solar cell applications.

Keywords: Polyaniline, monoclinic, vibrational bands, Tauc plot, optoelectronic.

1. INTRODUCTION:

Thin films have attracted considerable attention in science and technology due to their widespread applications in electronics, optoelectronics, sensors, and energy-related devices. A thin film is typically defined as a solid layer of material with thickness ranging from a few nanometers to several micrometers deposited on a suitable substrate. Owing to their reduced dimensionality, thin films often display properties that differ significantly from their bulk counterparts, including changes in electrical conductivity, surface morphology, and optical absorption. These distinctive features make thin films highly suitable for use in solar cells, transparent electrodes, photodetectors, gas sensors, and electrochromic devices [1, 2]. Therefore, systematic studies of the structural and optical characteristics of thin films are essential to optimize their performance for targeted applications.

Among the diverse thin film fabrication techniques, the Chemical Bath Deposition (CBD) method has become particularly attractive. CBD is a solution-based deposition process in which thin films are formed by controlled precipitation of materials from a supersaturated solution onto a substrate. Compared to

advanced methods such as pulsed laser deposition (PLD) or molecular beam epitaxy (MBE), CBD is relatively simple, cost-effective, and suitable for large-area coating. Importantly, CBD allows fine control over film thickness, morphology, and stoichiometry by adjusting deposition parameters such as precursor concentration, bath temperature, pH, and deposition time [2, 3]. Because of these advantages, CBD has been widely employed in the preparation of metal oxides, conducting polymer films, and hybrid organic–inorganic composites.

Conducting polymers, particularly Polyaniline (PANI), have emerged as highly versatile materials for electronic and optoelectronic devices. PANI is distinguished by its unique doping mechanism, wherein its electrical conductivity can be modulated through protonic or oxidative doping. This feature allows reversible transitions between insulating and conducting states, making PANI especially suitable for gas sensors, electrochromic devices, and supercapacitors [3]. It also exhibits good environmental stability, strong optical absorption in the visible region, and facile synthesis in various morphological forms. Nevertheless, its practical use is limited by issues such as moderate mechanical strength and thermal stability [4]. To overcome these limitations, hybridization with inorganic materials, such as metal oxides, is considered a promising strategy.

One of the most studied inorganic oxides for such hybrid systems is Tungsten trioxide (WO_3). WO_3 is an n-type semiconductor with a band gap ranging from 2.6 to 3.2 eV depending on synthesis conditions. It is well known for its electrochromic behavior, high refractive index, optical modulation capabilities, and environmental stability (Yao et al., 2021). WO_3 thin films are widely applied in electrochromic smart windows, photocatalysts, sensors, and energy conversion devices. WO_3 often suffers from low electrical conductivity, which restricts its applicability in certain electronic and optoelectronic devices [5, 6]. To address this, coupling WO_3 with conducting polymers such as PANI is a widely explored approach.

The WO_3–PANI hybrid thin films combine the unique advantages of both constituents: the good electrical conductivity and processability of PANI with the excellent electrochromic and optical properties of WO_3. Studies have reported that such hybrid films exhibit enhanced charge transport, superior electrochromic contrast, and improved stability compared to their individual counterparts [6, 7]. WO_3–PANI composites have shown promise as sensitive layers in gas sensors due to synergistic effects between the oxide and polymer phases [8]. To fully exploit their potential, however, it is decisive to systematically investigate the structural and optical properties of these films.

Structural analysis provides information about crystallinity, phase composition, and microstructure, which directly influence charge transport and film stability. Similarly, optical studies, including band gap evaluation, absorption spectra, and determination of optical constants, are critical for understanding light–matter interactions and for designing devices such as solar cells, photodetectors, and electrochromic displays [3, 9]. The use of the cost-effective CBD method to fabricate WO_3–PANI thin films further enhances their technological feasibility for large-scale applications. Therefore, the present study focuses on the preparation of WO_3–PANI thin films by CBD and the detailed investigation of their structural and optical properties to assess their potential in energy and optoelectronic applications.

2. EXPERIMENTAL PROCEDURE:

WO_3–PANI thin films were prepared on microscopic glass substrates by the chemical bath deposition (CBD) method. Initially, the glass substrates were cleaned with acetone and distilled water, to remove surface contaminants and ensure good film adhesion. The deposition bath was prepared by dissolving tungsten nitrate hexahydrate in distilled water as the precursor of WO_3. Aniline monomer was distilled prior to use and dissolved in 1 M HCl to obtain a protonated solution, into which ammonium persulfate (APS) was added as the oxidizing agent to initiate in-situ oxidative polymerization of aniline. The tungsten precursor solution and the protonated aniline solution were mixed in desired proportions under constant stirring, and the bath was maintained at normal room temperature and pressure. The cleaned substrates were vertically immersed in this bath, where simultaneous oxidative polymerization of aniline and precipitation of WO_3 occurred, leading to the formation of uniform WO_3–PANI thin films on the

substrate surface. After 2 minutes of time, the films were withdrawn, rinsed thoroughly with distilled water to remove loosely adhered particles, and dried at room temperature. Finally, the deposited films were annealed at moderate temperature at 100°C to improve film adhesion, enhance crystallinity, and ensure structural stability [8, 9]. The resultant WO_3–PANI films were used for structural and optical characterizations.

3. RESULT AND DISCUSSION:

Figure 1 shows the FESEM micrograph of the WO_3–PANI thin film recorded at a magnification of 50,000×. The FESEM image reveals a highly agglomerated microstructure composed of irregularly shaped particles with both spherical and plate-like morphologies. The measured grain sizes range from ~34.55 nm to ~920.2 nm, indicating a broad size distribution. The smaller nanograins appear to be closely packed and interconnected, while the larger flake-like structures form layered clusters, suggesting heterogeneous nucleation and growth during the chemical bath deposition process [10, 11]. Such a morphology provides a high surface-to-volume ratio, which is beneficial for enhancing charge transport and interfacial interactions.

$$Sw = 6/\rho d \qquad \text{(Eq. 1)}$$

Where, 6 – constant, d- diameter of particle and ρ- density of material.

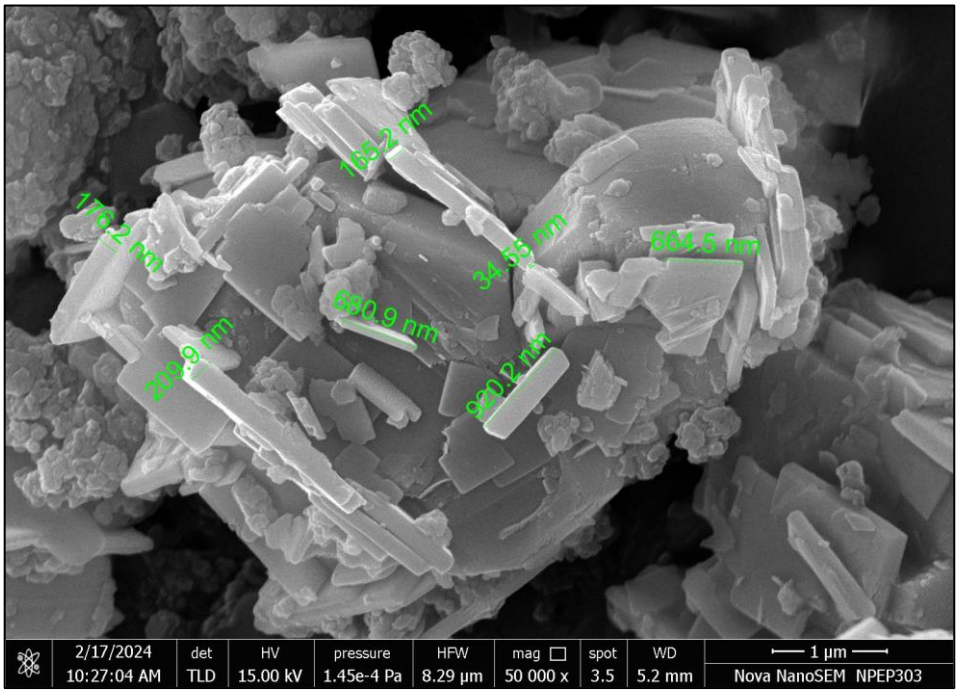

Figure 1: FESEM image of WO_3–PANI thin film

These microstructural observations are consistent with the Brunauer–Emmett–Teller (Eq. 1) analysis [12], which estimated the specific surface area of the WO_3–PANI thin film to be 3.68 m^2/g. The relatively high surface area confirms that the porous nature seen in FESEM contributes significantly to enhanced interfacial interactions. The rough and porous surface texture observed in the film can facilitate adsorption of gas molecules and efficient light absorption, making the WO_3–PANI composite thin films suitable for optoelectronic, photocatalytic, and battery applications. The observed microstructural features also confirm the successful integration of WO_3 crystallites within the PANI matrix, leading to the formation of a uniform hybrid film [13, 14].

Fig. 2 shows the EDX (Energy Dispersive X-ray) spectrum of the WO_3–PANI thin film, confirming the elemental composition of the deposited material. The spectrum exhibits prominent peaks corresponding to carbon (C), oxygen (O), and tungsten (W), which are the key constituents of the WO_3–PANI composite. The

strong carbon signal originates from the polyaniline (PANI) matrix, while the oxygen and tungsten peaks confirm the successful formation of tungsten oxide (WO_3) within the film [14, 15].

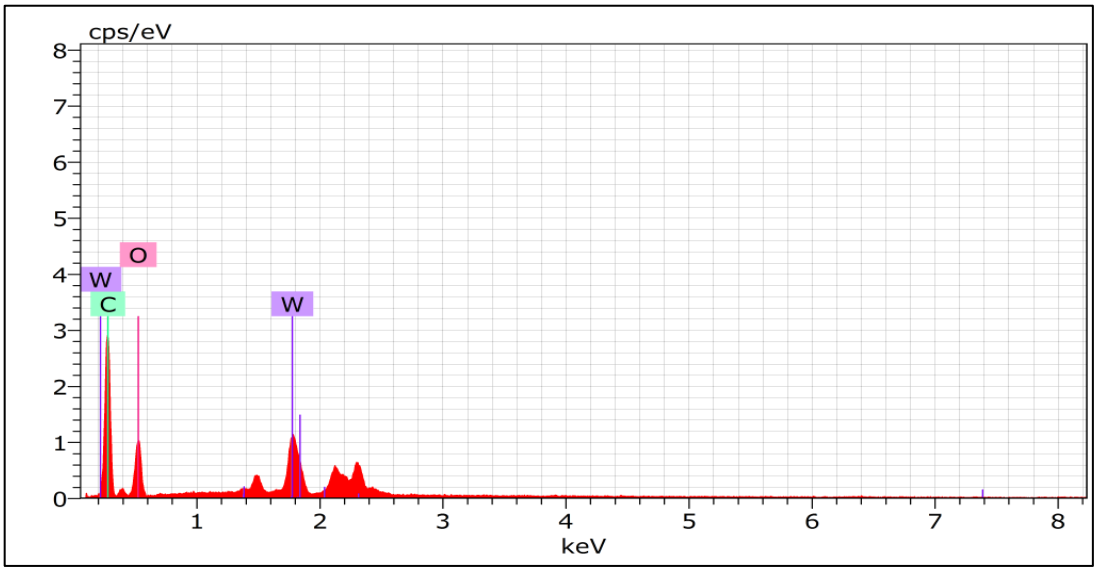

Figure 2: EDX spectra of WO_3–PANI thin film

The relative intensities of the peaks indicate the dominant presence of carbon, followed by tungsten and oxygen, which is in agreement with the EDX quantitative analysis values (C ≈ 48.68 wt.%, W ≈ 30.25 wt.%, O ≈ 21.07 wt.%). The absence of extraneous impurity peaks demonstrates the high purity of the synthesized thin film. These results validate the effective incorporation of both organic (PANI) and inorganic (WO_3) phases in the composite and support the formation of a uniform hybrid structure [15].

The X-ray diffraction (XRD) pattern of the WO_3–PANI thin film reveals important insights into its crystalline structure and phase composition. Distinct diffraction peaks are observed at 2θ values of 23.1°, 24.3°, 26.6°, 33.5°, and 34.1°, which correspond to the (002), (200), (120), (202), and (220) planes of monoclinic WO_3, respectively, in agreement with the standard JCPDS card No. 83-0950 [16]. The sharpness and intensity of these peaks confirm the successful formation of well-defined WO_3 crystallites within the composite [17].

$$D = (0.9\,\lambda\,)/(\beta\, Cos\, \theta) \quad \text{(Eq. 2)}$$

Where,

D – Crystallite or particle size, λ – Wavelength, θ – Angle of incidence, β – Full width at the half maximum (FWHM)

The crystallite size, calculated using the Debye–Scherrer equation (Eq. 2), and it is found to be 15.6 nm, suggesting that the film possesses a nanocrystalline nature.

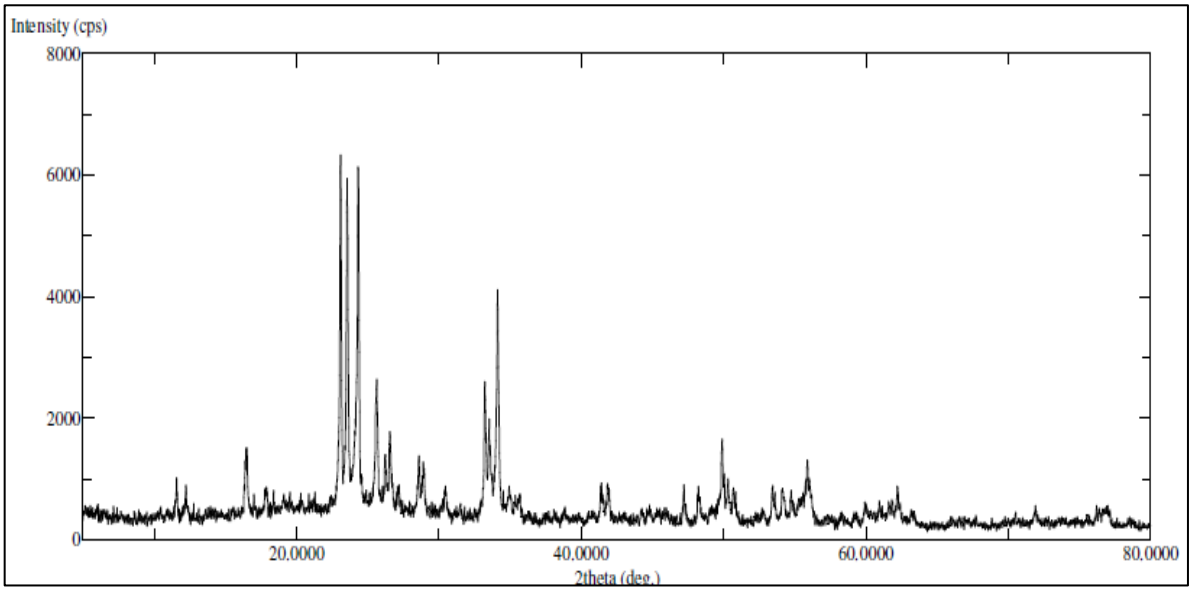

Figure 3: XRD spectra of WO_3–PANI thin film

The characteristic WO_3 reflections, a broad hump is observed in the region of 20°–30°, which is attributed to the semi-crystalline ordering of polyaniline (PANI). Since PANI does not possess a specific JCPDS reference due to its predominantly amorphous character, this broad feature is typically reported as evidence of short-range chain ordering in the polymer backbone. The coexistence of sharp WO_3 peaks and the broad halo of PANI confirms the formation of an organic–inorganic hybrid thin film, where WO_3 nanocrystals are uniformly embedded within the PANI matrix. Such a structural arrangement is advantageous as it combines the high crystallinity and stability of WO_3 with the conducting network of PANI, thereby enhancing interfacial charge transport, optical response, and overall film performance for potential optoelectronic and sensing applications [15, 17].

Figure 4 shows the FTIR spectrum of the WO_3–PANI thin film in the wavenumber range of 4000–500 cm^{-1}, which confirms the presence of functional groups associated with both polyaniline (PANI) and tungsten oxide (WO_3).

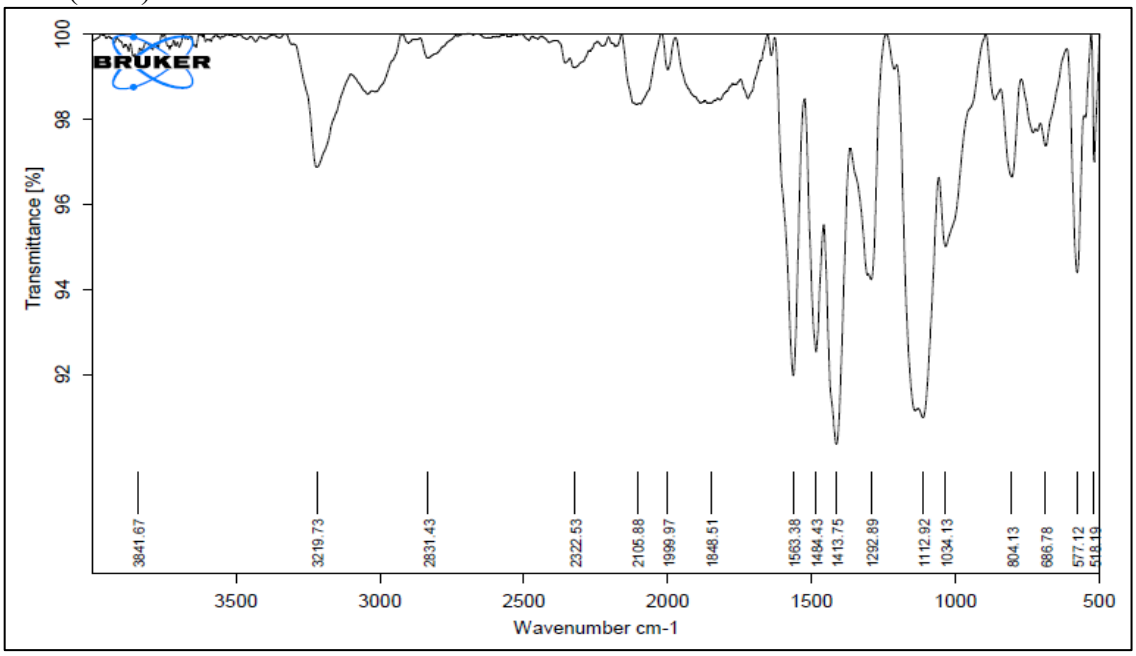

Figure 4: FTIR spectra of WO_3–PANI thin film

The broad absorption band observed around 3219–3341 cm^{-1} corresponds to the N–H stretching vibrations of PANI, while the weak band near 2841 cm^{-1} can be assigned to C–H stretching. The peaks at 1563 cm^{-1} and 1483 cm^{-1} are attributed to C=C stretching vibrations of quinoid and benzenoid rings of polyaniline, respectively, which indicate the conducting emeraldine salt form of PANI. The band around 1292 cm^{-1} corresponds to C–N stretching vibrations of the secondary aromatic amine, while the peak near 1112 cm^{-1} is associated with in-plane bending vibrations of C–H groups [9, 11]. A distinct band around 1034 cm^{-1} further supports the presence of C–N stretching in the PANI backbone. Importantly, strong absorption peaks below 900 cm^{-1}, particularly near 884, 677, and 577 cm^{-1}, correspond to W–O–W stretching vibrations, confirming the incorporation of WO_3 into the composite film. The presence of both organic (PANI) and inorganic (WO_3) vibrational modes in the spectrum validates the successful formation of a hybrid WO_3–PANI thin film. These characteristic vibrational features suggest strong interaction between the conducting polymer and the oxide matrix, which can enhance the structural stability and functional performance of the film in optical and electronic applications [14, 16].

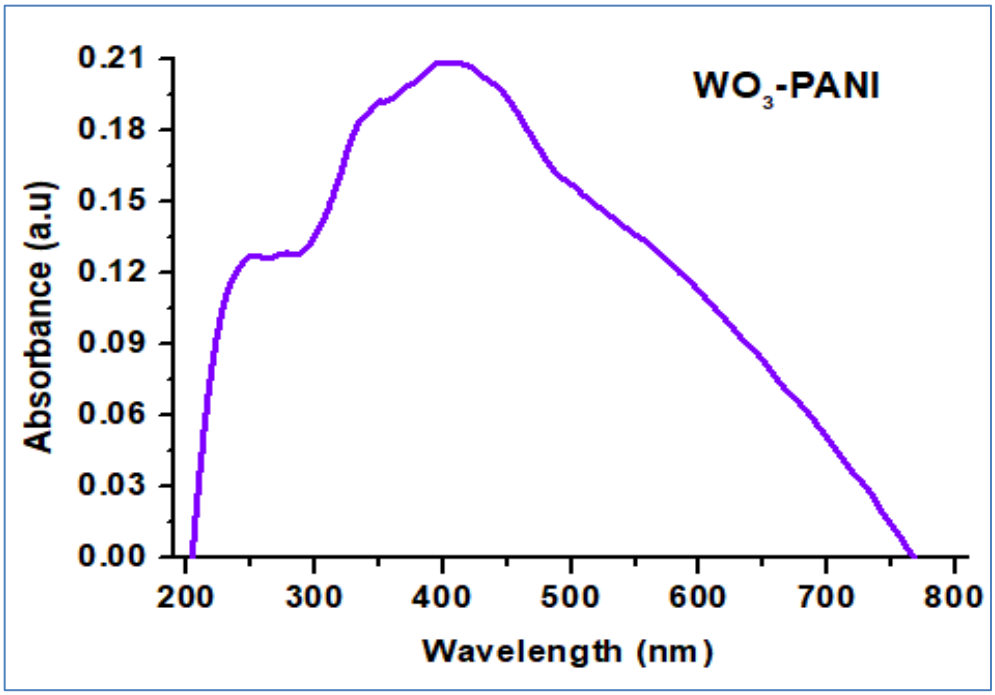

Figure 5: Absorbance versus wavelength spectra of WO_3–PANI thin film

Figure 5 presents the UV–Vis absorbance spectrum of the WO_3–PANI thin film in the wavelength range of 200–800 nm. The spectrum shows a strong absorption in the UV and visible regions, with a broad absorption peak centered around ~400 nm. This broad band is attributed to the combined contributions of WO_3 and PANI. For WO_3, the absorption in the UV region corresponds to charge transfer transitions from O 2p to W 5d states, while the visible absorption arises due to its semiconductor band gap [9, 15]. In the case of PANI, the absorption peaks are typically associated with π–π* transitions of the benzenoid rings (near 320–350 nm) and polaron–π* transitions of the conducting emeraldine salt form (around 400–420 nm). The broadening of the peak in the composite thin film suggests strong interaction between WO_3 nanoparticles and the PANI matrix, which enhances light absorption over a wider range [19, 20]. The absorption edge of the film is found near ~390 nm, from which the optical band gap can be estimated using Tauc's plot and was calculated to be ~3.2 eV. The strong absorption in the visible region along with the wide band gap indicates that the WO_3–PANI thin film possesses semiconductor characteristics, making it suitable for optoelectronic applications [14, 16].

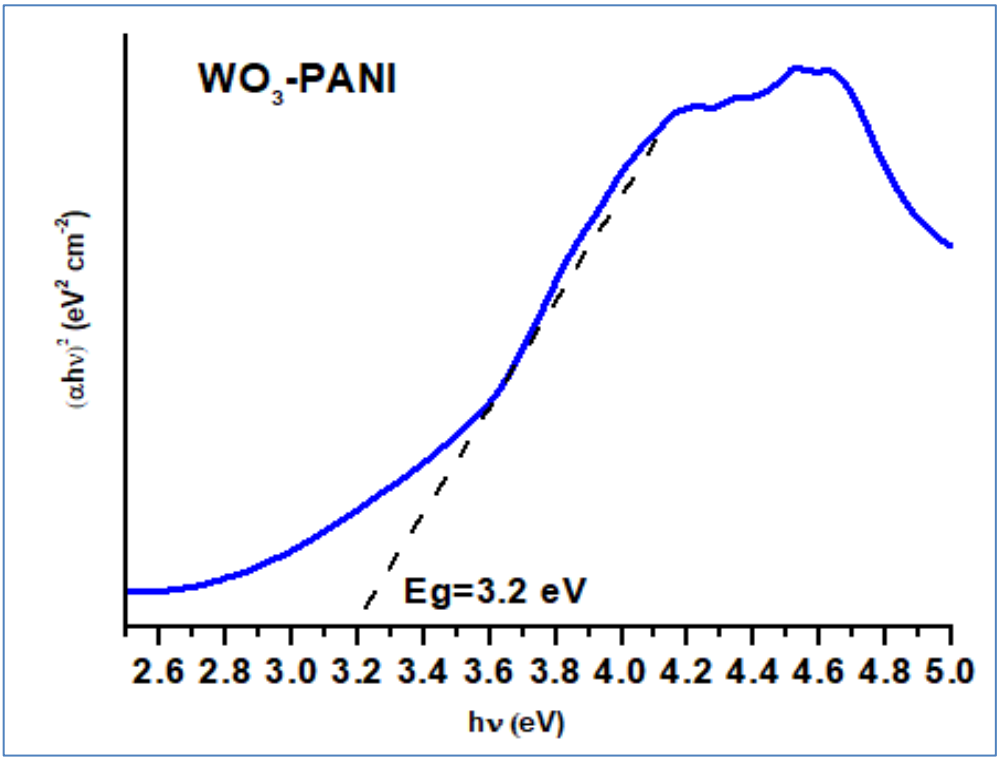

Figure 6: Tauc plot of WO_3–PANI thin film

Figure 6 illustrates the Tauc plot of the WO_3–PANI thin film, which is used to estimate the optical band gap energy of the material. The graph shows a linear region in the higher energy side of the spectrum, and by extending this straight portion to intersect the energy axis, the optical band gap value was determined [17, 18]. The optical band gap was calculated using the Tauc relation (Eq. 3).

$(\alpha h\nu)^2 n = A (h\nu - Eg)$ (2.7)

Where,

α is the absorption coefficient of the material,

hν is the photon energy (with *h* being Planck's constant and ν being the frequency of light),

A is a proportionality constant,

Eg is the optical band gap energy and

n is an exponent that depends on the type of electronic transition.

The band gap of the WO_3–PANI thin film was found to be about 3.2 eV. This value is in close agreement with reported band gap values of tungsten oxide-based composites, confirming its semiconducting nature [18, 19]. The presence of polyaniline in the composite enhances absorption in the visible region while maintaining a wide band gap, which is beneficial for optoelectronic, electrochromic, and photocatalytic applications [20]. The structural and optical outcomes of WO_3–PANI thin film are tabulated in Table 1.

Table 1: Structural and optical outcomes of WO_3–PANI thin films.

XRD				**FESEM**	**EDX**	**UV**
2θ (°)	FWHM (β)	Intensity (a.u.)	Crystallite size (nm)	Surface area (m^2/g)	Elements (wt. %)	Band gap (eV)
24.30	0.541	4968	15.66	3.68	C-48.68 W-30.25 O-21.07	3.2

CONCLUSIONS:

WO_3–PANI thin films were successfully synthesized on glass substrates using the chemical bath deposition (CBD) method, and their structural and optical properties were comprehensively investigated. XRD analysis confirmed the formation of nanocrystalline monoclinic WO_3 with a crystallite size of 15.66 nm, along with a broad hump characteristic of semi-crystalline PANI, thereby validating the formation of an organic–inorganic hybrid structure. FESEM images revealed agglomerated nanostructures with porous morphology, while BET analysis indicated a specific surface area of 3.68 m^2/g, suggesting enhanced surface activity and interfacial interactions. EDX results verified the elemental composition, showing the successful incorporation of tungsten, oxygen, and carbon within the composite. FTIR spectra further confirmed the hybrid structure by exhibiting characteristic vibrational modes of both WO_3 and PANI. Optical studies demonstrated strong absorption in the UV–visible region, with the Tauc plot estimating a direct band gap of 3.2 eV, highlighting the semiconducting nature of the film. The combination of nanocrystalline WO_3 and conducting PANI in a hybrid thin film structure offers favorable structural stability, enhanced light absorption, and potential for use in optoelectronic, photocatalytic, electrochromic, and solar cell applications.

Acknowledgment:

The authors gratefully acknowledge the Research Centre in Electronic Science, L. V. H. College, Panchavati, Nashik, India, for providing the necessary laboratory facilities and support to carry out this work. The authors also extend their sincere thanks to the Central Instrumentation Facility (CIF), Pune, for providing advanced characterization facilities that were crucial for the successful completion of this research study.

REFERENCES:

1. Beygisangchin, M., et al. (2021). Preparations, properties, and applications of polyaniline thin films: A review. Polymers, 13(12), 2003.
2. He, W., Zhang, H., Chen, H., Zhou, Q., & Fang, X. (2020). Bilayer polyaniline–WO_3 thin-film sensors sensitive to NO_2. ACS Omega, 5(2), 873–880.
3. Mohamedkhair, A. K., et al. (2021). Tuning structural properties of WO_3 thin films for photoelectrocatalytic water oxidation reaction. Catalysts, 11(3), 381. https://doi.org/10.3390/catalysts11030381
4. Valentová, H., Stejskal, J., Trchová, M., Prokeš, J., & Kopecký, D. (2010). Mechanical properties of polyaniline. Synthetic Metals, 160(7–8), 832–839.
5. Yao, Y., Sang, D., Zou, L., Wang, Q., & Liu, C. (2021). A review on the properties and applications of WO_3 nanostructure-based optical and electronic devices. Nanomaterials, 11(8), 2136. https://doi.org/10.3390/nano11082136
6. Zhang, J., Tu, J., Zhang, D., Qiao, Y., Xia, X., Wang, X., & Gu, C. (2011). Multicolor electrochromic polyaniline–WO_3 hybrid thin films: One-pot molecular assembling synthesis. Journal of Materials Chemistry, 21(44), 17316–17324.
7. He, W., Zhang, H., Chen, H., Zhou, Q., & Fang, X. (2020). Bilayer polyaniline–WO_3 thin-film sensors sensitive to NO_2. *ACS Omega*, *5*(2), 873-880.
8. Nwanya, A. C., Jafta, C. J., Ejikeme, P. M., Ugwuoke, P. E., Reddy, M. V., Osuji, R. U., ... & Ezema, F. I. (2014). Electrochromic and electrochemical capacitive properties of tungsten oxide and its polyaniline nanocomposite films obtained by chemical bath deposition method. *Electrochimica Acta*, *128*, 218-225.
9. Yuksel, R., Durucan, C., & Unalan, H. E. (2016). Ternary nanocomposite SWNT/WO3/PANI thin film electrodes for supercapacitors. *Journal of Alloys and Compounds*, *658*, 183-189.

10. Wang, Y. D., Zhang, S., Ma, C. L., & Li, H. D. (2007). Synthesis and room temperature photoluminescence of ZnO/CTAB ordered layered nanocomposite with flake-like architecture. *Journal of luminescence*, *126*(2), 661-664.
11. Wang, J., & Zhang, D. (2013). One-Dimensional Nanostructured Polyaniline: Syntheses, Morphology Controlling, Formation Mechanisms, New Features, and Applications. *Advances in Polymer Technology*, *32*(S1), E323-E368.
12. Tupe, U. J., Zambare, M. S., Patil, A. V., & Koli, P. B. (2020). The binary oxide NiO–CuO nanocomposite based thick film sensor for the acute detection of hydrogen sulphide gas vapours. *Materials Science Research India*, *17*(3), 260–269
13. Najafi-Ashtiani, H., & Bahari, A. (2016). Optical, structural and electrochromic behavior studies on nanocomposite thin film of aniline, o-toluidine and WO3. *Optical Materials*, *58*, 210-218.
14. Hsini, A., Naciri, Y., Laabd, M., Bouziani, A., Navío, J. A., Puga, F., ... & Albourine, A. (2021). Development of a novel PANI@ WO3 hybrid composite and its application as a promising adsorbent for Cr (VI) ions removal. *Journal of Environmental Chemical Engineering*, *9*(5), 105885.
15. He, W., Zhao, Y., & Xiong, Y. (2020). Bilayer polyaniline–WO3 thin-film sensors sensitive to NO2. *ACS omega*, *5*(17), 9744-9751.
16. Qiu, Y., Xu, G. L., Kuang, Q., Sun, S. G., & Yang, S. (2012). Hierarchical WO3 flowers comprising porous single-crystalline nanoplates show enhanced lithium storage and photocatalysis. *Nano research*, *5*(11), 826-832.
17. Nithya, G., Kumar, K. N., Shaik, H., Reddy, S., Sen, P., Prakash, N. G., & Ansari, M. A. (2024). Simulation and deposition of Tungsten oxide (WO3) films using DC sputtering towards UV photodetector for high responsivity. *Physica B: Condensed Matter*, *695*, 416555.
18. Phogat, P., Rawat, S., Thakur, J., Jha, R., & Singh, S. (2025). Influence of metal ion doping on the photo-electrochemical detection performance of WO_3. *Sensors and Actuators A: Physical*, *382*, 116150.
19. Zhang, J., Tu, J. P., Zhang, D., Qiao, Y. Q., Xia, X. H., Wang, X. L., & Gu, C. D. (2011). Multicolor electrochromic polyaniline–WO3 hybrid thin films: one-pot molecular assembling synthesis. *Journal of Materials Chemistry*, *21*(43), 17316-17324.
20. Lin, D. S. (2004). Absorbance Behavior of Polyaniline-Poly (Styrenesulfonic Acid) Complexes and Tungsten Oxide. *Journal of the Chinese Chemical Society*, *51*(6), 1279-1286.